第 36 卷第 2 期 无 机 化 学 学 报 Vol.36 No.2
2020 年 2 月 CHINESE JOURNAL OF INORGANIC CHEMISTRY 385-391

油分散性核壳 Fe_3O_4@MnO 纳米复合材料的合成及其对氧化环化反应的催化性能

杨清香 雷李玲 王青青 王芳草 王 聪 董梦果 李银萍 陈志军*
(郑州轻工业学院材料与化学工程学院,河南省表面与界面科学重点实验室,郑州 450002)

摘要:采用两相种子介导法以锰油酸为前驱体制备了一种新型油溶性核壳结构 Fe_3O_4@MnO 纳米复合材料,直径约为 15 nm。所制备的具有核壳结构的纳米复合材料是单分散且均匀的。该产物对 2-羟基苯乙酮和 1,2-二氨基苯的氧化环化反应表现出高且可循环的催化活性。与在环化反应中使用的其他报道的催化剂相比,所制备的 Fe_3O_4@MnO 纳米复合材料绿色、廉价且更适合于大规模工业应用。

关键词:Fe_3O_4@MnO;纳米复合材料;磁性材料;油分散性;氧化环化反应;催化
中图分类号:O643 **文献标识码**:A **文章编号**:1001-4861(2020)02-0385-07
DOI:10.11862/CJIC.2020.032

Synthesis and Catalytic Performance for Oxidative Cyclization Reaction of Oil-Dispersible Core-Shell Fe_3O_4@MnO Nanocomposites

YANG Qing-Xiang LEI Li-Ling WANG Qing-Qing WANG Fang-Cao
WANG Cong DONG Meng-Guo LI Yin-Ping CHEN Zhi-Jun*
(*School of Material and Chemical Engineering, Henan Provincial Key Laboratory of Surface and Interface Science, Zhengzhou University of Light Industry, Zhengzhou* 450002, *China*)

Abstract: A new type oil-soluble core-shell structure Fe_3O_4@MnO nanocomposites with diameter about 15 nm was prepared through two-phase seed mediate method with Mn-oleate precursors. The as-prepared nanocomposites with core-shell structure were monodispersed and uniform. The products exhibited high and recyclable catalytic activity for the oxidative cyclization reaction of 2-hydroxyacetophenone and 1,2-diaminobenzene. Compared with other reported catalysts used in this kind of cyclization reaction, the as-prepared Fe_3O_4@MnO nanocomposites are green, cheap and more suitable for large scale industrial applications.

Keywords: Fe_3O_4@MnO; nanocomposite; magnetic materials; oil-dispersible; oxidative cyclization reaction; catalytic

0 Introduction

In recent years, phase segregated hetero structures, in which two or more inorganic domains are combined through a small interfacial area, have attracted increasing attention[1]. Hetero structured magnetic nanoparticles (NPs) are fantastic materials due to their combined features of magnetism and multi-functionalities[2]. There are many magnetic hybrids that have been reported, such as precious metals/Fe_3O_4, CdS/FePt, CdSe/Fe_3O_4, MnO/Fe_3O_4, and γ-Fe_2O_3/metal sulfides, which show novel properties and potential applications that cannot be achieved solely with single component nanocrystals[3-9].

收稿日期:2019-08-20。收修改稿日期:2019-12-09。
国家自然科学基金(No.20976168,21271160,21401170)和 2018 年度河南省高等学校青年骨干教师资助计划(No.2018GGJS088)资助。
*通信联系人。E-mail:chenzj@zzuli.edu.cn

Manganese oxides are widely used as catalysts[10-11], magnetic resonance imaging contrast agents[12], and electrode material[13]. Mn-oleate and Mn-acetate have been used as precursor in the synthesis of MnO NPs[14-17]. In homogeneous medium, the Mn-O cubane systems have been well developed for water oxidation to mimic the biological system. In 2014, Kim reported that MnO nanocrystals were synthesized and used as catalyst[18], due to the small size, it was difficult to separate the catalyst from the reaction system and to recycle. So it is an efficient way to combine MnO with magnetic particles. Lee et al.[1] prepared various Fe_3O_4/MnO hybrid nanocrystals with Mn-acetate precursors, and the surface of the hybrid nanocrystals were water soluble. Oil-dispersible Fe_3O_4/MnO hybrid nanocrystals fabricated with Mn-oleates as precursors have not been reported yet. In this work, oil-dispersible Fe_3O_4 nanocrystals were fabricated via decomposition of Fe $(CO)_5$ metal-oleates (reported by Peng[19] and Hyeon[20] in 2004). According to the principles of "like dissolves like", we supposed if using Mn-oleate as precursor to grow MnO shell on the surface of oil-dispersible Fe_3O_4 nanocrystals, controllable structure of Fe_3O_4/MnO nanocomposites with hydropholic/oil-dispersible surface would be obtained, and further study on the catalytic property of this kind of Fe_3O_4/MnO nanocomposites would be interested.

1 Experimental

Chemicals: Manganese(Ⅱ) chloride tetrahydrate ($MnCl_2\cdot 4H_2O$, 98%) and ferric chloride hexahydrate ($FeCl_3\cdot 6H_2O$, 99%) were purchased from Tianjin Kemiou Chemical Reagent Co., Ltd. and used as received. 2-Hydroxyacetophenone ($C_8H_8O_2$, 98%), 1,2-diaminobenzene ($C_6H_8N_2$, 98%), 1-octadecene ($C_{18}H_{36}$, 90%), 1-octadecene ($C_{18}H_{36}$, 90%) and sodium oleate ($C_{18}H_{33}NaO_2$, 97%) were purchased from Shanghai darui fine chemical Co., Ltd. All chemicals were used as received without any further purification.

Characterization: Wide-range powder X-ray diffraction (XRD) measurements were carried out on an AXS D8 X-ray diffraction spectrometer (Bruker, Germany) with a Cu $K\alpha$, λ =0.154 18 nm radiation (U=60 kV, I=60 mA) at scan rate of 0.04°·s^{-1} in region of 2θ from 10° to 80°. Infrared (IR) absorption spectra of the nanocomposites were recorded in the range of 400~4 000 cm^{-1} on a Nicolet (Impact 410) spectrometer with KBr pellets (5 mg of sample in 500 mg of KBr). The size and morphology of the products were examined by scanning electron microscopy (SEM, JEOL JSM-6490 LV, 5 kV, 10 mA) and transmission electron microscopy (TEM, JEOL JEM-2100 working at 200 kV). Magnetic measurement was performed on a LS7307-9309 type high field vibrating sample magnetometer.

Preparation of Fe_3O_4@MnO nanocomposites: Oil-dispersible Fe_3O_4 nanocrystals were prepared through previously reported procedure through the thermal decomposition of Fe-oleic acid complexes at high temperature[17]. Typically, 5 mL Fe_3O_4 (0.01 g) solution in hexane was added into a flask, then 2.48 g Mn-oleate complex, 0.122 g sodium oleate and 100 mL 1-octadecene were added, respectively. After stirred for 12 h, the mixture suspension was heated to 320 ℃ and stirred for 5 h, then cooled down to room temperature. The products were washed by hexane for several times, separated by the external magnetic field, and dried under vacuum at 60 ℃ for 12 h.

Catalytic activity test: The experiments were performed in an autoclave reactor. 0.396 2 g (2.91 mmol) of 2-hydroxyacetophenone, 0.629 4 g (5.82 mmol) of 1,2-diaminobenzene, 0.005 g of Fe_3O_4@MnO nanocomposites were dissolved in 15 mL DMF (*N*,*N*-dimethylformamide). The mixture was transferred to a Teflon-lined autoclave, which was then heated at 130 ℃ for 6 h. After cooling to room temperature, the reaction mixture was filtered, washed with saturated aqueous $NaHCO_3$ solution, and extracted with dichloromethane. The organic layer was concentrated under reduced pressure and analyzed by GC-MS (TRACE GC Ultra).

2 Results and discussion

2.1 Characterization of Fe_3O_4@MnO nanocomposites

As shown in Fig.1a, Fe_3O_4 nanoparticles are spherical particles with diameter of about 10 nm,

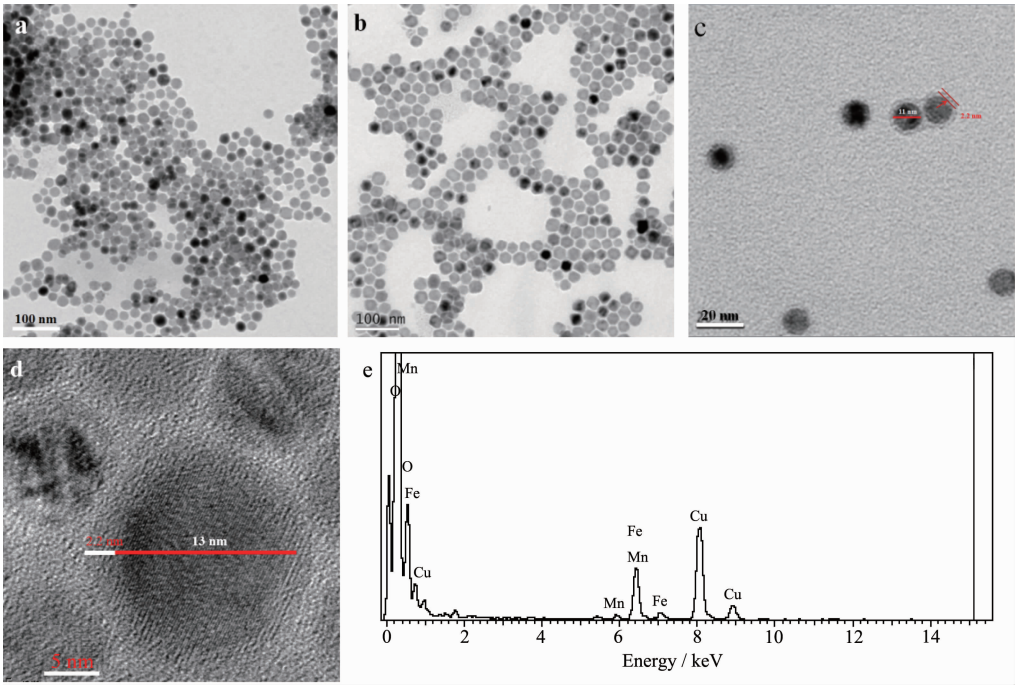

Fig.1　TEM images of (a) Fe_3O_4 nanoparticles, (b) MnO nanoparticles, and (c) Fe_3O_4@MnO nanocomposites; (d) High resolution-TEM images and (e) EDX microanalysis spectrum of Fe_3O_4@MnO nanocomposites

which are nearly monodispersed. Fig.1b shows TEM image of MnO nanoparticles, which have octahedral shape with diameter of about 20 nm. Fig.1(c,d) showed TEM images of core-shell structured Fe_3O_4@MnO nanocomposites with diameter of about 15 nm, which were monodispersed, demonstrating that the oleate-capped Fe_3O_4@MnO nanocomposites prepared by this method have a uniform size distribution and can be dispersed excellently in nonpolar solvent such as cyclohexane. Fig.1d shows Fe_3O_4 core with the darker region in the center (about 10 nm) and the lighter MnO shell (about 2.2 nm). Mn, Fe, and O were detected in the EDX (energy dispersive X-ray) spectrum, which can be attributed to Fe_3O_4@MnO nanocomposites (Fig.1e).

In order to determine the crystal structure and the composition of the as-prepared samples, phase analyses of the X-ray diffraction (XRD) measurements were carried out for bare Fe_3O_4 nanoparticles, bare MnO nanoparticles and Fe_3O_4@MnO nanocomposites. Fig.2a showed the XRD patterns of the Fe_3O_4, the diffraction peaks at 18.1°, 30.1°, 35.1°, 37.1°, 43.1°, 53.4°, 56.9°, 62.5° and 73.9° were respectively corresponded to (111), (220), (311), (222), (400), (422), (511), (440) and (533) crystal planes, which were well matched with face-centered cubic phase of Fe_3O_4 (PDF No.65-3107). The XRD analysis confirmed the formation of MnO, as shown in Fig.2b. The five diffraction peaks at 2θ values of 34.9°, 40.6°, 58.7°, 70.2°, and 73.7° can be indexed to the diffraction of (111), (200), (220), (311), and (222) planes of standard cubic MnO (PDF No.07-0230), indicating the formation of MnO[21-22]. As shown in Fig.2c, the diffraction peak of the Fe_3O_4@MnO composite corresponds to the diffraction peaks of pure Fe_3O_4 and pure MnO, indicating that the prepared composite is a composite structure in which the core

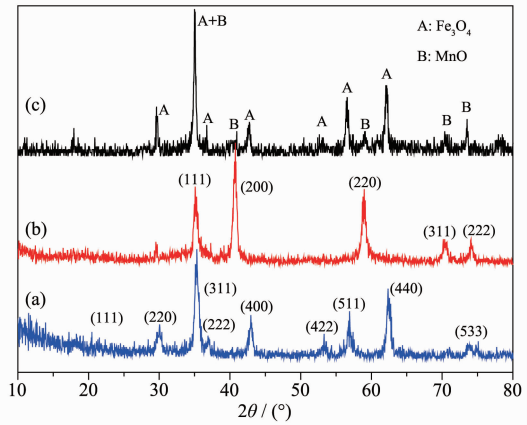

Fig.2　XRD patterns of (a) Fe_3O_4 nanoparticles, (b) MnO nanoparticles, and (c) Fe_3O_4@MnO nanocomposites

is Fe_3O_4 and the shell is MnO. The crystal phase structure of Fe_3O_4 did not change during the formation of the composite.

To analyze the product composition and chemical states of the elements, XPS characterizations are conducted and the results are given in Fig.3(a~c). In the wide-scan survey spectrum (Fig.3a), the XPS peaks for Fe2*p*, Mn2*p*, O1*s*, and C1*s* were observed, indicating the presence of Fe, Mn, O, and C elements in the sample. In the Mn2*p* spectrum shown in Fig.3b, two characteristic peaks at 641.4 and 652.9 eV can be attributed to the Mn2$p_{3/2}$ and Mn2$p_{1/2}$ of MnO, respectively[23]. Fig.3c illustrates the Fe2*p* high-resolution XPS spectra of the sample, two characteristic peaks at 709.0 and 722.8 eV can be attributed to the Fe2$p_{3/2}$ and Fe2$p_{1/2}$ of Fe_3O_4, respectively. Fe2$p_{3/2}$ and Fe2$p_{1/2}$ states can reveal the presence of Fe^{3+} and Fe^{2+} [24]. And the exact content of Fe and Mn was determined by atomic absorption spectrophotometry. The specific result was 20:1 (n_{Fe}:n_{Mn}).

To further confirm the formation of Fe_3O_4@MnO nanocomposites, IR analysis was conducted to reveal the surface nature of Fe_3O_4@MnO, as shown in Fig.4a. The bands appeared at 2 909 and 2 845 cm^{-1} corresponded to stretching vibration modes of -CH_2- and -CH_3, respectively. The absorption bands appeared at 1 606 and 1 401 cm^{-1} could be ascribed to O-C=O and -C=C- stretching vibration modes, respectively. The peak at 556 cm^{-1} was Fe-O stretching vibration. The results suggest the presence of residual oleic acid chains on the surface of Fe_3O_4@MnO nanocomposites[25]. As shown in Fig.4, highly stable Fe_3O_4@MnO nanocomposites were dispersed in hexane, and did not penetrate into water system. The result demonstrated that Fe_3O_4@MnO nanocomposites were oil-dispersible and modified with hydrophobic oleic acid chains.

The magnetic properties of the Fe_3O_4@MnO nanocomposite was investigated by using a high field vibrating sample magnetometer. As shown in Fig.4b, the saturation magnetization value of Fe_3O_4@MnO was 47 emu·g^{-1}, which was much larger than MnO (1.1 emu·g^{-1})[19] at 300 K and 20 000 Oe. The coercive force of Fe_3O_4@MnO was close to 0, which was also different from MnO, the literature reports that m-MnO nanocrystals NCs are paramagnetic[26]. The increase of the saturation magnetization of the Fe_3O_4@MnO enabled

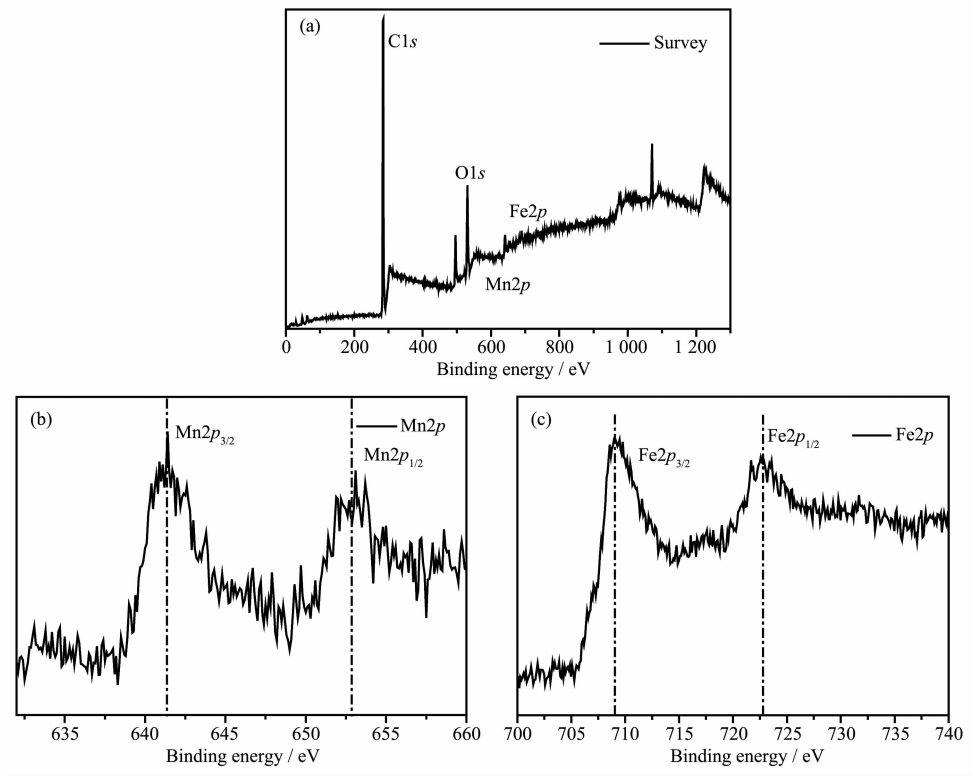

Fig.3 XPS image of the Fe_3O_4@MnO: (a) survey, (b) Mn2*p*, and (c) Fe2*p*

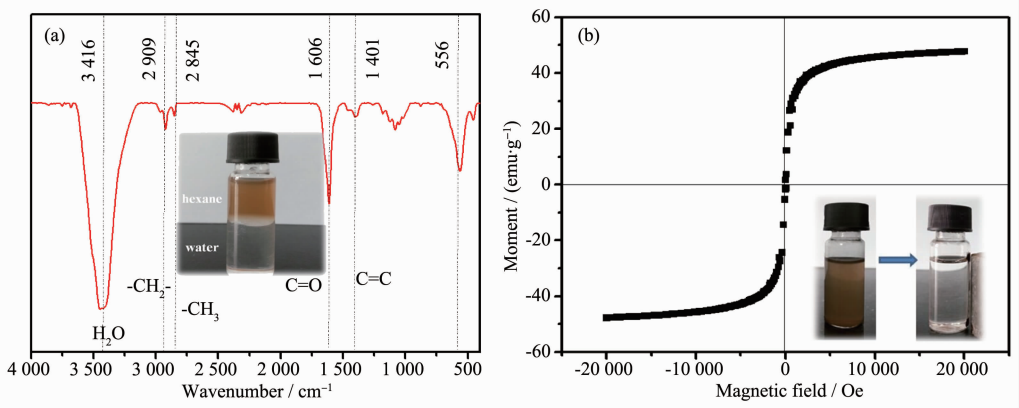

Fig.4　(a) IR spectra of Fe_3O_4@MnO nanocomposites (Inset: photograph of Fe_3O_4@MnO nanocomposites dispersed in hexane/water solution); (b) Magnetization hysteresis of Fe_3O_4@MnO nanocomposites (Inset: photographs of magnetic separation and redispersion)

the catalyst to be magnetically separated under an external magnetic field within few seconds after the catalytic reaction is completed, which facilitates recovery and regeneration (Inset in Fig.4b). In addition, the separated particles were easily re-dispersed under slight shaking and could maintain a relatively stable suspension state and catalytic activity for several months, which was also superior to other catalysts. This is essentially important for the convenient reuse of Fe_3O_4@MnO nanocomposites.

2.2　Catalytic activity

MnO as catalyst usually possesses high activity. The hybrid of MnO nanoparticles with magnetic support may render them to be a practical recyclable nanocatalyst. We first employed Fe_3O_4@MnO nanocomposites as catalysts for the catalytic oxidative cyclization of 2-hydroxyacetophenone with 1,2-diaminobenzeneto to generate the corresponding quinoxaline derivative without any additives. The cyclization reaction of 2-hydroxyacetophenone and 1,2-diaminobenzeneto for the synthesis of 2-phenylquinoxaline was carried out over the MnO, Fe_3O_4, Fe_3O_4/MnO mixture, and Fe_3O_4@MnO composite, and the results are given in Table 1. For comparison, the catalytic activities of bare Fe_3O_4 nanoparticles and bare MnO nanoparticles were performed in the same conditions. As shown in Table 1, Fe_3O_4@MnO nanocomposites showed good catalytic performance. The catalytic results revealed that Fe_3O_4@MnO nanocomposites (Yield: 91.43%) exhibited higher catalytic performance than the Fe_3O_4 nanoparticles (Yield: 81.51%) and Fe_3O_4/MnO mixture (Yield: 86.61%), and the catalytic activities of which is almost the same as MnO nanoparticles (Yield: 91.91%).In order to study the optimal conditions for the use of the catalyst, we investigated the effects of temperature, catalyst dosage and catalytic time on the conversion. The results show that the conversion of 6 h in the presence of 0.005 g of Fe_3O_4@MnO nanocomposite was 91.43%. The amount of the composite catalyst was increased to 0.01 g, and the conversion was 91.51%, and there was no significant increase. We speculated that the product of the catalytic reaction can be quickly separated from the surface of the catalyst during the catalytic process. Therefore, increasing the amount of catalyst has no significant effect on the conversion.

Table 1　Different catalysts for the synthesis of quinoxaline

Catalyst	Solvent	Temperature / ℃	Time / h	Yielda / %
MnO	DMF	130	3	91.91
Fe_3O_4	DMF	130	3	81.51
Fe_3O_4+MnO (physical mixture)	DMF	130	3	86.61
Fe_3O_4@MnO	DMF	130	3	91.43

[a] Determined by GC-MS

The effect of temperature on the synthesis of quinoxaline was investigated in a range of 60~180 ℃ and the results are shown in Fig.5a. The maximum yield of the quinoxaline was obtained at 130 ℃. Below 130 ℃, the catalytic activity was lower, which may be due to the fact that the active site on the surface of the catalyst was occupied by the reactant diamine, and there was not enough active site for the cyclization reaction. It is assumed that the amine is adsorbed on the acidic sites of the catalyst, thereby blocking the active sites required for the cyclization reaction [27]. The high reaction temperature above 130 ℃ result in low yield, which enhanced the formation of polyalkyl products[28]. Fig.5b is a plot of yield versus time. It can be seen that the yield values tended to equilibrate when the catalytic reaction time was greater than 6 h.

The catalysts for the cyclization catalytic reaction reported in the literature were compared. The results are shown in Table 2[29]. It can be seen that the catalyst not only has good catalytic activity, but also facilitates quick and convenient separation under an external magnetic field.

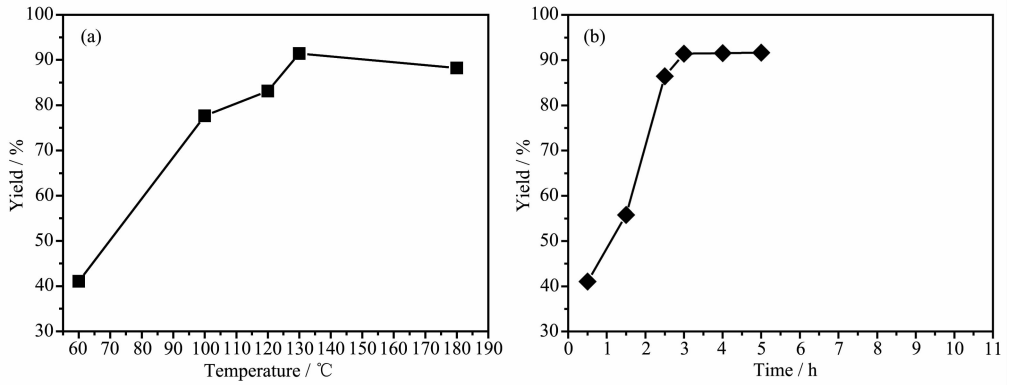

Fig.5 Relationship of conversion vs (a) temperature and (b) time

Table 2 Activities of as-prepared catalyst compared with other catalyst

Catalyst	Solvent	T / ℃	Time / h	Yield / %	Reference
MnO	CH_2Cl_2	100	3	86	[28]
MnO_2	CH_2Cl_2	100	3	88	[28]
Mn	CH_2Cl_2	100	3	78	[28]
Fe_3O_4@MnO	DMF	130	3	91	This work

The recyclability and repeated catalytic activities of Fe_3O_4@MnO nanocomposites were demonstrated.

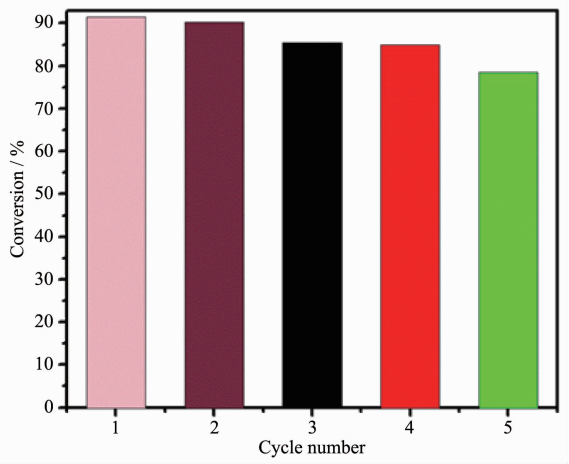

Fig.6 Recycling catalytic activity of Fe_3O_4@MnO nanocomposites

The as-prepared Fe_3O_4@MnO nanocomposites catalyst can be efficiently recovered and recycled in the reaction mixtures by magnetic separation. The renewable catalytic activity was investigated by performing the oxidative cyclization five times using Fe_3O_4@MnO nanocomposites. Fig.6 showed the conversion for each run which was measured by GC-MS analysis. The conversion droped slightly after each cycle, and it maintained at 78% at the five cycle.

3 Conclusions

Oil-soluble core-shell Fe_3O_4@MnO nanocomposites with diameter about 15 nm was fabricated with $Fe(CO)_5$ metal-oleates and Mn-oleate precursors via two-phase seed mediate method. Compared with previously

reports in which prepared Fe_3O_4/MnO composites with Mn-acetate, using Mn-oleate as precursor, we obtained oil-soluble, monodispersed and size-uniform nanocomposites. We first used this kind of structured Fe_3O_4@MnO nanocomposites as catalyst for the oxidative cyclization reaction of 2-hydroxyacetophenone with 1,2-diaminobenzene to produce quinoxaline. The results demonstrated that the as-prepared Fe_3O_4@MnO nanocomposites exhibited good recyclability, high stability and high catalytic activity.

Acknowledgements: This work was supported by grants from the Natural Science Foundation of China (Grants No. 20976168, 21271160, 21401170) and 2018 Henan Provincial College Young Key Teachers Funding Scheme (Grant No. 2018GGJS088).

References:

[1] Lee K S, Anisur R M, Kim K W, et al. *Chem. Mater.*, **2012**, **24**(4):682-687

[2] Conte M P, Sahoo J K, Abulhaija Y M, et al. *ACS Appl. Mater. Interfaces*, 24,**10**(3):3069-3075

[3] Fanani M L, Wilke N. *Biochim. Biophys. Acta Biomembr.*, **2018**,**1680**(10):1972-1984

[4] Jiao T F, Liu Y Z, Wu Y T, et al. *Sci. Rep.*, **2015**,**5**:12451-12461

[5] Xu C J, Xie J, Ho D, et al. *Angew. Chem. Int. Ed.*, **2008**,**47**(1):173-176

[6] Xiao D L, Hui L, Hua H, et al. *New Carbon Mater.*, **2014**,**71**(1):343-343

[7] Kwon K W, Shim M. *J. Am. Chem. Soc.*, **2005**,**127**(29):10269-10275

[8] Gao J H, Zhang W, Huang P B, et al. *J. Am. Chem. Soc.*, **2008**,**130**(12):3710-3711

[9] Chen M L, Gao Z W, Chen X M, et al. *Talanta*, **2018**,**182**:433-442

[10]Zhang G F, Zhang Q H, Cheng T T, et al. *Langmuir*, **2018**, **34**(13):4052-4058

[11]Fang Z D, Zhang K, Liu J, et al. *Water Sci. Eng.*, **2017**,**10**(4):326-333

[12]Lu Y, Zhang L, Li J, et al. *Adv. Funct. Mater.*, **2013**,**23**(12):1534-1546

[13]Chen L D, Zheng Y Q, Zhu H L. *J. Mater. Sci.*, **2018**,**53**(2):1346-1355

[14]Puglisi A, Mondini S, Cenedese S, et al. *Chem. Mater.*, **2010**,**22**(9):2804-2813

[15]Yin M, O′Brien S. *J. Am. Chem. Soc.*, **2003**,**125**(37):10180-10181

[16]Souri M, Hoseinpour V, Shakeri A, et al. *IET Nanobiotechnol.*, **2018**,**12**(6):822-827

[17]Bulut A, Yurderi M, Alal O, et al. *Adv. Powder Technol.*, **2018**,**29**(6):1409-1416

[18]Kim A, Shin D, Kim M, et al. *Eur. J. Inorg. Chem.*, **2014**, **2014**(8):1279-1283

[19]Jana N R, Chen Y, Peng X. *Chem. Mater.*, **2004**,**16**(20):3931-3935

[20]Park J, An K H, Wang Y, et al. *Nature Mater.*, **2004**,**3**(12):891-895

[21]Jiang H, Hu Y J, Guo S J, et al. *ACS Nano*, **2014**,**8**(6):6038-6046

[22]Zhong K F, Xia X, Zhang B, et al. *J. Power Sources*, **2010**, **195**(10):3300-3308

[23]Wu Q L, Jiang M L, Zhang X F, et al. *J. Mater. Sci.*, **2017**, **52**(11):6656-6669

[24]He Z S, Wang K, Wang S S, et al. *ACS Appl. Mater. Interfaces*, **2018**,**10**(13):10974-10985

[25]Gamelin T C, Stemmler D R, Mandal T L, et al. *J. Am. Chem. Soc.*, **1998**,**120**:8724-8738

[26]Kim A, Shin D, Kim M, et al. *Eur. J. Inorg. Chem.*, **2014**, **2014**(8):1279-1283

[27]Chen D T, Zhang L, Chen Y, et al. *J. Catal.*, **1994**,**146**(1):257-263

[28]Hölderich W F, Röseler J, Heitmann G, et al. *Catal. Today*, **1997**,**37**(4):353-366

[29]Kim, Park S Y, Chung K H, et al. *Chem. Commun.*, **2005**, **36**(10):1321-1323